Available online at www.sciencedirect.com
ScienceDirect
Journal of Power Sources 178 (2008) 238–247
JOURNAL OF POWER SOURCES
www.elsevier.com/locate/jpowsour

Process modification for coating SnO_2:F on stainless steels for PEM fuel cell bipolar plates

Heli Wang *, John A. Turner, Xiaonan Li, Glenn Teeter

National Renewable Energy Laboratory 1617, Cole Boulevard, Golden, CO 80401, USA

Received 22 October 2007; received in revised form 3 December 2007; accepted 4 December 2007
Available online 14 December 2007

Abstract

Our previous procedure for depositing SnO_2:F on stainless steels for interfacial contact resistance (ICR) reduction and as a protective coating for metal bipolar plates was modified by pre-etching and coating characterization. Only ferrite stainless steels acquired a good quality SnO_2:F coating. The modified SnO_2:F coating decreased the ICR over our previous coating results, confirming the beneficial effect of the pre-etching; however, the corrosion resistance we obtained was significantly reduced.

For the pre-etched and coated AISI444 and AISI446, both dynamic and potentiostatic polarizations revealed that the corrosion resistance of the modified coated steels is not as good as that obtained with the original coating process. The pre-etched and coated AISI444 showed higher currents in the polymer electrolyte membrane fuel cell (PEMFC) anode environment, as compared with earlier coated (original) AISI444 results. It took 10–50 min to reach a stabilized current for the pre-etched and coated AISI446; moreover, the stable currents are higher than those for original coated AISI446. Inductive coupled plasma (ICP) analysis for dissolved metallic ions in the test solutions was in agreement with the polarization results. Additionally, both the polarization and ICP analysis results indicate that the PEMFC cathode environment is more corrosive to the coated steels (especially AISI444) than the PEMFC anode environment.

The Auger electron spectroscopy (AES) investigation showed that the pre-etched and coated AISI444 had heavy dissolution in the PEMFC cathode environment, confirming that for this process it has enhanced corrosion over the PEMFC anode environment. Both coated AISI444 and coated AISI446 showed cracks and peel-off of the modified coating after the polarization. This is apparently the source for the higher anodic currents in the polarization curves as compared to our original process for coating the steels. The conclusion is that both the corrosion resistance in PEMFC environments and the adhesion of the modified SnO_2:F coating are challenges for further development.
Published by Elsevier B.V.

Keywords: Bipolar plate; Stainless steels; Ferrite; Tin oxide; PEMFC

1. Introduction

Major challenges for the use of stainless steels as bipolar plates in a polymer electrolyte membrane fuel cell (PEMFC) include the corrosion resistance in the fuel cell anode and cathode environments and the interfacial contact resistance (ICR) between the gas diffusion layer and the bipolar plate [1–3]. However, because stainless steels have a high mechanical strength, high chemical stability, a wide range of alloy compositions, low cost and a number of available pathways for high-volume high-speed production, they are the best candidates for PEMFC bipolar plates, especially for automotive applications [1–11]. Unfortunately, the contact resistance with the bare stainless steels is high, resulting in a reduction of the fuel cell performance. Additionally, metal ions coming from the corrosion of the metallic bipolar plates may contaminate the membrane [12,13], thus decreasing membrane conductivity and lowering the efficiency of the fuel cell [14].

There have been a number of different approaches to try and improve the stainless steel surface so as to have a lower ICR and better corrosion resistance. Wind et al. [13] showed that for a 1000 h test, a gold-coated 316L matched the performance of graphite. Others reported similar results with gold-coated 316L [15]. Pt coated 316 also had excellent behavior in single cell tests [16]. Not too surprisingly, precious metals significantly reduced the contact resistance. Nonetheless, it is apparent that

* Corresponding author. Tel.: +1 303 275 3858; fax: +1 303 275 2905.
E-mail address: heli_wang@nrel.gov (H. Wang).

0378-7753/$ – see front matter. Published by Elsevier B.V.
doi:10.1016/j.jpowsour.2007.12.010

the high cost and limited availability of these precious metals eliminates their commercial viability. Conductive polymers have also been proposed by different groups [17–19]. The long-term stability of these polymers at elevated temperatures under the corrosive PEMFC environments is still a challenge. Previously, a thermal nitridation process was developed [20] and applied to a Ni–50Cr model alloy; this showed excellent corrosion resistance and low ICR [21,22]. Moreover, surface modification via thermal nitridation of a lower cost ferritic AISI446 steel resulted in a chemical change of the native passive film of the alloy, significantly decreasing the ICR and improving the corrosion resistance in simulated PEMFC environments [23]. Tian et al. recently reported an approach using plasma-assisted nitridation to lower the treatment temperature and increase the productivity [24]. However, these approaches all have limitations and may not be viable in all cases, which leads us to investigate other possibilities. Our approach in searching for coating/substrate combinations is to identify cost-effective substrate materials with high corrosion resistance in PEMFC environments and then apply a coating that is both corrosion resistance and having low interfacial contact resistance. In this approach, the coating does not need pin-hole free since any exposure of the substrate alloy will result in the passivation and further active corrosion of the substrate is eliminated. Previously, we reported the results for a fluorine-doped SnO_2 (SnO_2:F) coating on austenite and ferrite stainless steels for PEMFC bipolar plate applications. In general, the corrosion resistance for the coated steels in simulated PEMFC environments was significantly improved with the 0.6 μm thick SnO_2:F coating, though the substrate steel played a very important role in coating stability [25,26]. However, that coating process added an additional resistance to the resistance of the previous air-formed film and the total ICR of the coated steels was increased. In this paper we will describe our efforts to optimize the coating process to lower the ICR on selected steels.

2. Experimental

2.1. Materials and electrochemistry

Stainless steels plates of 349, 2205, AISI444 and AISI446 were provided by J&L Specialty Steel, Inc., now part of Allegany Ludlum. The chemical compositions have been given elsewhere [9–11]. The alloy plates were cut into samples of 2.54 cm × 1.25 cm (1.0 in. × 0.5 in.). The samples were rubbed with #600 grit SiC abrasive paper, rinsed with acetone, and dried with nitrogen gas.

The fluorine-doped SnO_2 (SnO_2:F) coating was prepared via a low-pressure chemical vapor deposition (LPCVD) process [27], using ultrahigh-purity (UHP) tetramethyltin (TMT, Morton International) and bromotrifluoromethane ($CBrF_3$) as the tin and fluorine precursors, respectively; UHP-grade oxygen was used as the oxidizer. Detailed procedures are reported elsewhere [25,26]. To obtain a lower ICR, the deposition procedure was modified. The term "modified" is used to differentiate from the "original" coating process. For the modified process, $CBrF_3$ was used to etch off some of the stainless steels' air-formed film. This was done by introducing only $CBrF_3$ into the deposition chamber immediately before starting the deposition process. Etching times between 0.3 and 4 min were tried and the deposition time ranged from 15 to 27 min. We observed that the coatings on the austenitic and duplex steels samples showed poor adhesion and surface wrinkles and were easily peeled-off. This is in contrast with our previous coating process where good coating adhesion was obtained. In the current study, good coatings were only obtained with the ferritic stainless steels AISI444 and AISI446. Thus most of the following discussion and results will concentrate on the pre-etched and coated AISI444 and AISI446.

The electrode preparation process for the electrochemical measurements has been described previously [9–11]. A 1 M H_2SO_4 + 2 ppm F^- solution was prepared to simulate an aggressive PEMFC environment. All electrochemical experiments were conducted at 70 °C and the solution was bubbled thoroughly with either hydrogen gas (for simulating a PEMFC anode environment) or pressurized air (for simulating a PEMFC cathode environment) prior to and during the electrochemical measurements. The setup for the electrochemical measurements has been described in detail [9–11].

2.2. Interfacial contact resistance

All ICR measurements were carried out at room temperature and in an air environment. The method for conducting the ICR measurements has been previously described [9]. Briefly, two pieces of conductive carbon paper were sandwiched between the stainless steel sample and two copper plates. A current of 1.000 A was provided via the two copper plates and the total voltage drop was registered. Gradually increasing the compaction force gives the dependence of the total resistance on the compaction force. The ICR value of the carbon paper/copper plate interface ($R_{C/Cu}$) was compensated for via a calibration, so in this report we give only the ICR values for the carbon paper/stainless steel interface. Both fresh and SnO_2:F coated steels were investigated. Fresh steel samples were used to baseline the carbon paper/stainless steel interface resistance ($R_{C/SS}$). For the SnO_2:F coated steel samples, the interfacial contact resistance due to the uncoated backside was deducted from the previous measurements with the fresh steel samples, so only the ICR of the carbon paper/SnO_2:F coated steel interface ($R_{C/TO}$) was used in this report.

2.3. Characterizations

The SnO_2:F coating's composition and the depth profile was determined by Auger electron spectroscopy (AES) analysis and was carried out using a Phi670 Auger Nanoprobe with a chamber base pressure of 4.0×10^{-8} Pa (3×10^{-10} Torr). The depth profiles were obtained by sputtering with 3 keV argon ions with a current density of around 1 μA mm^{-2}, and a system pressure in the chamber of approximately 6.67×10^{-6} Pa (5×10^{-8} Torr). Based on the previous measurements, a reasonable estimate of the sputtering rate was approximately 35 nm min^{-1}.

Test solutions (80–100 ml) were collected after 7.5 h of potentiostatic polarization with both coated and uncoated steels, purged either with air or hydrogen gas. An inductive coupled

plasma (ICP) spectrometer was used to quantify the dissolved metallic ion species (Fe, Cr, Ni and Sn ions) in the solutions used for testing. The ICP system was a Varian Liberty 150 ICP Emission Spectrometer controlled by a PC. A standard solution, containing 100 ppm of each of the metal ions in 1 M H_2SO_4, was purchased from Inorganic Ventures, Inc. The estimated relative uncertainty for ICP analysis, mainly due to variability in the plasma, pump rate and nebulizer efficiency, is 5% [28].

3. Results and discussion

3.1. Modifying SnO_2:F deposition for lower ICR

The influence of the substrate was still an issue for this modified coating process. Though the same coating procedure was applied for ferritic, austenitic and duplex stainless steels, the coating on austenitic and duplex steels samples showed poor adhesion as evidenced by surface wrinkles and peeling. Good coatings were only obtained with the ferritic stainless steels AISI444 and AISI446 (Fig. 1). Seen on the coated 349 surface in Fig. 1 are many wrinkles, while the edges of the coated 2205 are partially peeled-off. In contrast, coated AISI444 and AISI446 give excellent-looking coatings. Since the austenite and ferrite steels have similar lattice parameters, the good coating adhesion on the ferrite stainless steels is likely related to the ferritic stainless steels body centered cubic (bcc) structure which is similar to the tetragonal structure of SnO_2:F (Fig. 2).

The ICR between the SnO_2:F coated stainless steel samples and the carbon paper was investigated as a function of compaction force (Fig. 3). The ICR values with uncoated steels and coated with the previous process [26] are also shown for comparison. With the original SnO_2:F coating, the ICR was increased due to the additional resistance of the native coating on the bare steels. With the modified SnO_2:F coating process, involving a pre-etch to remove that native coating, the ICR decreased. This is more evident in the lower compaction force region than in the higher one. Pre-etching then has a beneficial effect on the ICR. A possible explanation for the lowing ICR due to etching is that the etching procedure have several functions on the substrate surface, including surface cleaning, removing the native oxide film and increasing the surface roughness. All of these functions will contribute to the reduction of the ICR.

The modified coated AISI444 shows lower ICR values than AISI446, following the trend of the bare steels and the original coating process. This is an important improvement with ICR. Since we are not concerned with the transparency of the coating, a thicker coating and optimization of the etching process could be applied to improve the ICR further, as well as address some of the adhesion problems.

3.2. Dynamic polarization of SnO_2:F coated stainless steels

Dynamic polarization measurements in 1 M H_2SO_4 + 2 ppm F^- at 70 °C purged with H_2 indicates that the modified coated AISI444 has a polarization curve similar to those of the fresh steel and the original coated AISI444 (Fig. 4a). The critical passivating current (peak current for starting passivation) is almost

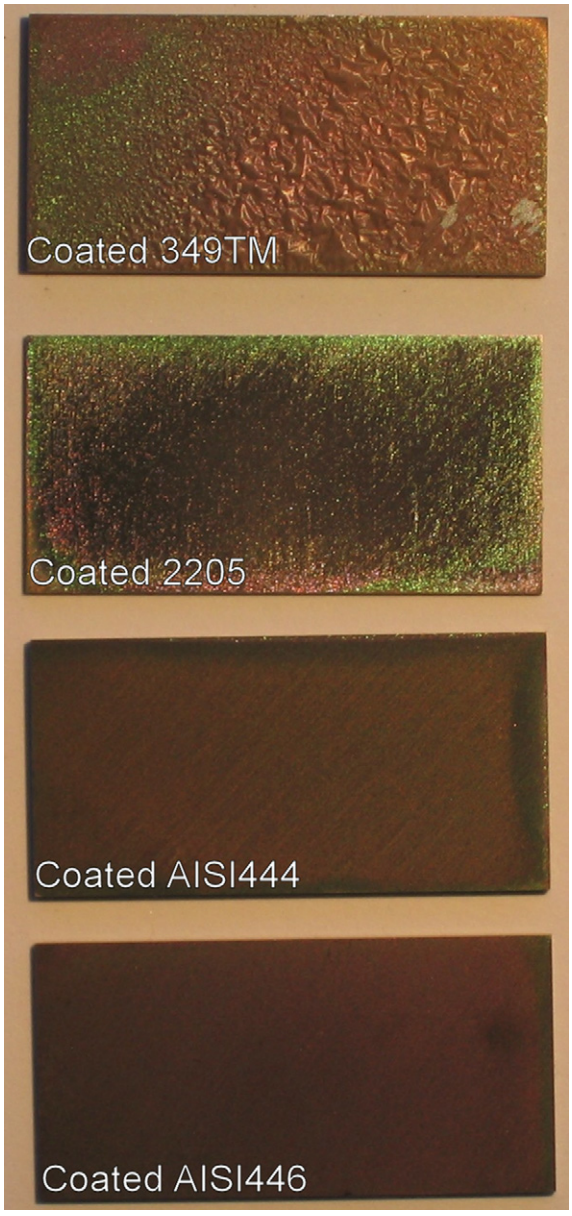

Fig. 1. Modified SnO_2:F coating on different substrate steels.

the same for the three curves, regardless of the coating process. Some slight differences however can be found in the passive region of the curves. The original coated AISI444 shows the lowest passivation current (the lowest current to maintain passivation) amongst the samples, suggesting the possible advantage of corrosion resistance for the original coated AISI444. The anode potential in PEMFC application (−0.1 V) is located inside the passivation region for all the three curves. At this potential in hydrogen-purged solution, fresh AISI444 has a current density of *ca.* 90 μA cm^{-2}, the original SnO_2:F coated AISI444 shows a current of *ca.* 55 μA cm^{-2}, and the modified coated AISI444 has a current of *ca.* 85 μA cm^{-2}. Comparing to US DOE target of 1 μA cm^{-2} [29], all of these currents are rather close and clearly too high.

Fig. 4b shows the dynamic polarization curves for fresh and coated AISI444 steels in the solution purged with air. Again,

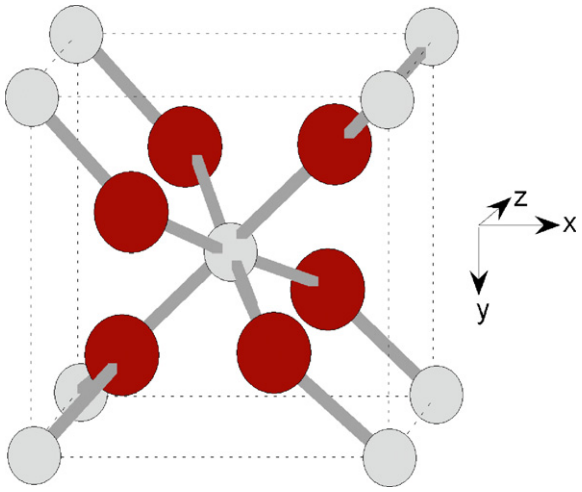

Fig. 2. Tetragonal lattice for SnO_2: $a = b = 4.738$ Å; $c = 3.188$ Å; $\alpha = \beta = \gamma = 90°$. O atom: bigger ball; Sn atom: smaller ball. (For interpretation of the references to color in this figure legend, the reader is referred to the web version of the article.)

the critical passivating currents are at the same level for the three curves, regardless of the coating conditions. However, the critical passivating potential (the potential corresponding to the critical passivating current peak) shifts anodically after the SnO_2:F coating. It is *ca.* −0.29 V for fresh AISI444, *ca.* −0.24 V for original coated AISI444, and *ca.* 0.01 V for modified coated AISI444. This shift is remarkable for the modified coated AISI444; additionally, the shape of the polarization curve is changed significantly. There are secondary current peaks in the curves for the fresh AISI444 and the original coated AISI444. These secondary current peaks are not seen in the curve for the modified coated AISI444. The cathode potential in the PEMFC application (0.6 V) is still located inside the passivation regions for all the three curves. Fresh AISI444 has a current density of *ca.* 20 μA cm^{-2} at 0.6 V in air-purged solution, the original SnO_2:F coated AISI444 shows a current of *ca.* 75 μA cm^{-2} at 0.6 V, and the modified coated AISI444 has a current of *ca.* 46 μA cm^{-2} at this potential, Fig. 4b. However, it should be mentioned that the dynamic polarization curve is not sufficient to predict the application of this coated alloy under PEMFC operating conditions.

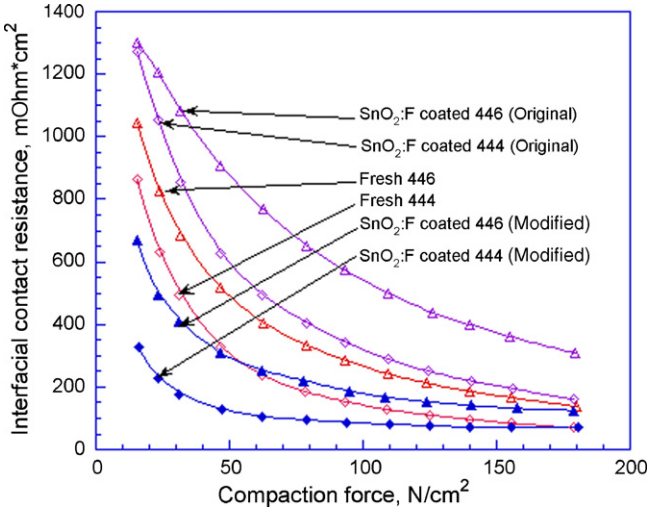

Fig. 3. Interfacial contact resistances for fresh and SnO_2 coated stainless steels and carbon paper at different compaction forces. Original: depositing directly without further surface preparation; modified: pre-etching before the deposition.

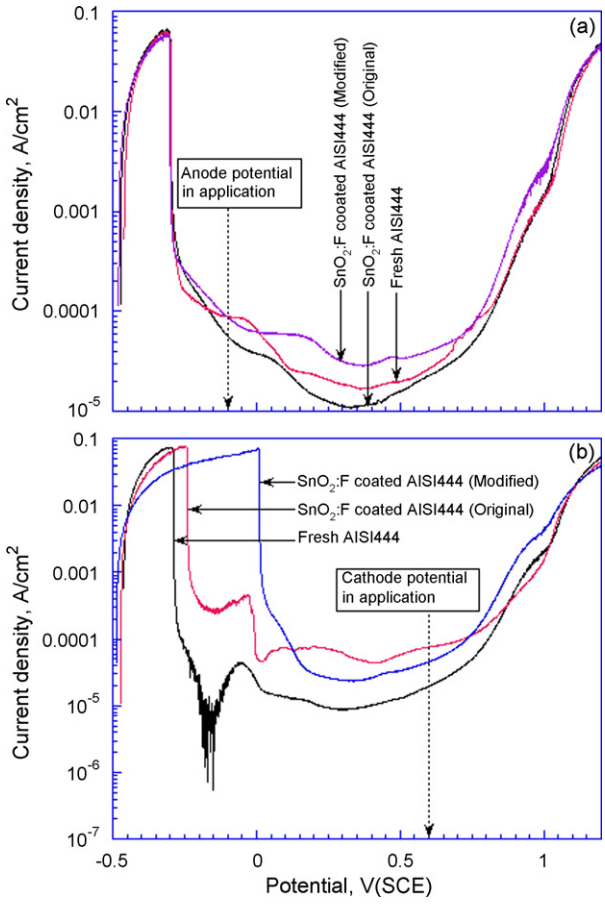

Fig. 4. Anodic behavior of fresh and SnO_2:F coated AISI444 stainless steels in 1 M H_2SO_4 + 2 ppm F^- at 70 °C purged with H_2 (a) or pressured air (b). The potentials in PEMFC application are marked. Original: depositing directly without further surface preparation; modified: pre-etching before the deposition.

Fig. 5 shows the polarization curves for modified coated AISI446 under the same conditions. In hydrogen-purged solution, the modified coating is rather different from that obtained from the non-pre-etched coating. The open circuit potential (OCP) of the original coated AISI446 shifts anodically to *ca.* 0.09 V as compared with *ca.* −0.22 V for fresh AISI446 under the same conditions. The OCP for modified coated AISI446 is at *ca.* −0.27 V, a cathodic shift compared with the fresh AISI446. This results in different polarization curves, Fig. 5a. Throughout the whole polarization region, the current for original coated AISI446 is reduced by over one order of magnitude, indicating improved corrosion resistance for the original SnO_2:F coating on AISI446. On the other hand, the current for the modified coated AISI446 shows an increase many times the current for the fresh AISI446, suggesting that there is a degrading effect of this coating in terms of corrosion resistance. The passive current for the modified coated AISI446 is higher than that for both the fresh steel and the previously coated one. The current for the modified coated AISI446 at the anode potential is also higher than the rest.

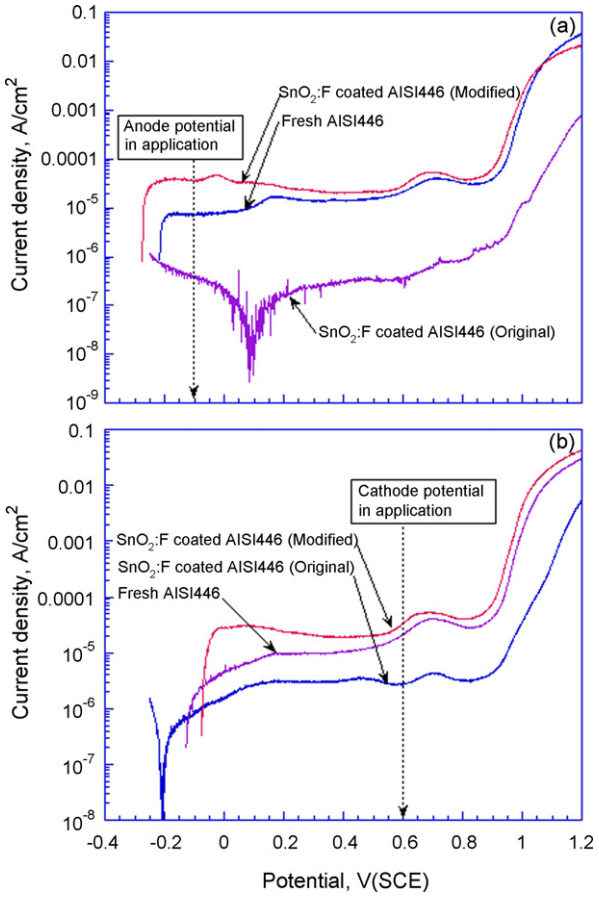

Fig. 5. Anodic behavior of fresh and SnO_2:F coated AISI446 stainless steels in 1 M H_2SO_4 + 2 ppm F^- at 70 °C purged with H_2 (a) or pressured air (b). The potentials in PEMFC application are marked. Original: depositing directly without further surface preparation; modified: pre-etching before the deposition.

For comparison, the currents at −0.1 V are *ca.* 7.0 μA cm^{-2} for fresh AISI446, *ca.* −0.4 μA cm^{-2} for original coated AISI446, and *ca.* 35 μA cm^{-2} for modified coated AISI446.

Fig. 5b gives the polarization curves in solution purged with pressured air; results similar to Fig. 5a are observed. The OCP for the fresh AISI446 in the air-purged solution is at *ca.* −0.13 V. The original coating process on AISI446 shifts the OCP in the cathodic direction to *ca.* −0.21 V, while the modified coated AISI446 shows a shift of the OCP in the anodic direction to *ca.* −0.07 V. Again, the passivation current increases for the modified coated AISI446. The current at the cathode potential is also increased with the modified coated AISI446. The currents at 0.6 V are *ca.* 20 μA cm^{-2} for fresh AISI446, *ca.* 2.7 μA cm^{-2} for the original coated AISI446, and *ca.* 34 μA cm^{-2} for modified coated AISI446, again confirming the decreased corrosion resistance in a PEMFC cathode environment for the pre-etched and coated steel.

3.3. Potentiostatic polarization of SnO_2:F coated stainless steels

Potentiostatic polarization measurements were used to evaluate further the performance of the modified SnO_2:F coating.

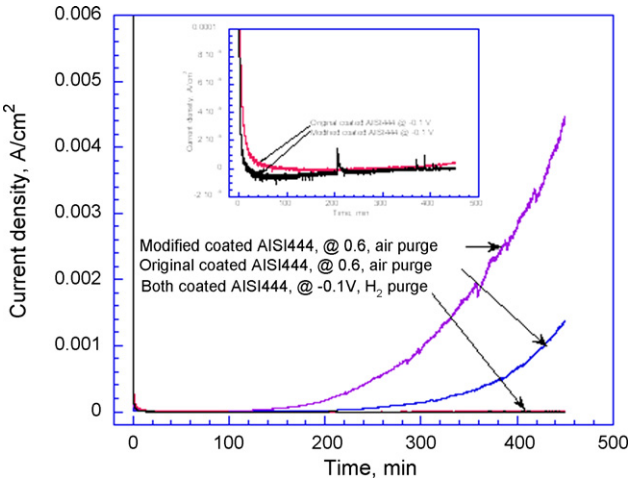

Fig. 6. Transient currents of SnO_2:F coated AISI444 stainless steels either at −0.1 V in 1 M H_2SO_4 + 2 ppm F^- at 70 °C purged with hydrogen gas or at 0.6 V in the solution purged with pressured air. Insert shows the details for the coated AISI444 at −0.1 V in 1 M H_2SO_4 + 2 ppm F^- at 70 °C purged with hydrogen gas.

Fig. 6 shows the transient currents of SnO_2:F coated AISI444 stainless steels either at −0.1 V in 1 M H_2SO_4 + 2 ppm F^- at 70 °C purged with H_2 gas or at 0.6 V in the same solution purged with pressured air. The insert shows the details for the coated AISI444 under hydrogen gas conditions.

As soon as a potential is applied, there is a sharp current decay for the coated AISI444 steels, regardless of the applied potential and the purge gas. In H_2-purged solution and at −0.1 V, very similar current–time curves are observed for the coated AISI444 steel samples, inset of Fig. 6. Both show an anodic–cathodic current changeover. For the original coated AISI444, this anodic–cathodic current transition occurs at *ca.* 80 min and it crosses back to anodic current again at *ca.* 260 min of polarization. A similar transition was reported previously [9]. The current is rather stable for the whole period. For the modified coated AISI444, the anodic–cathodic current transition occurs at *ca.* 20 min and the current crosses back to anodic again at *ca.* 380 min of polarization. Currents are in the range of *ca.* −1.0–4.0 μA cm^{-2} for original coated AISI444 and in the range of *ca.* −7.0–1.0 μA cm^{-2} for modified coated AISI444. While the current for the modified coated AISI444 is generally more negative (cathodic), it shows some current spikes during the measurement period. The current spikes could be related to the dissolution of surface film or similar issues, leading to concerns about the corrosion resistance of the modified coated AISI444 in the PEMFC anode environment.

When polarized at 0.6 V with the air purge, as soon as the potential is applied, the current decays rapidly for the coated AISI444, even faster than in the PEMFC anode environment. For the original SnO_2:F coated AISI444 steel polarized at 0.6 V, a stable current is reached after 10 min of polarization at a current level of *ca.* 3.0–5.0 μA cm^{-2} (Fig. 6). It remains stabile until *ca.* 160 min when a moderate current increase is observed. After 450 min, the current for the original coated AISI444 reaches *ca.* 1.40 mA cm^{-2}. Under the same condition, the current for the modified coated AISI444 is stable after *ca.* 20 min,

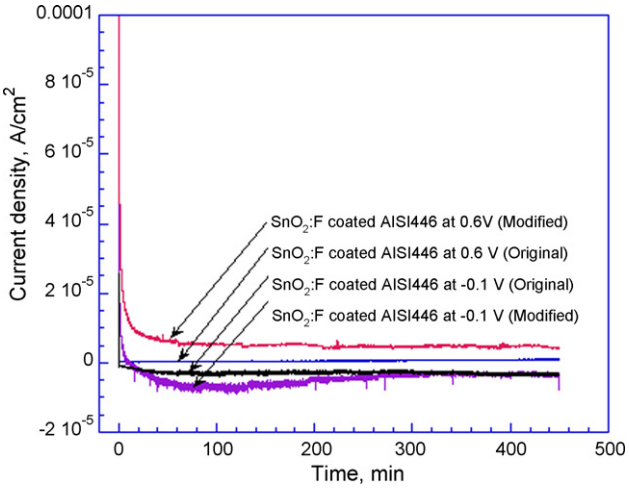

Fig. 7. Transient currents of SnO_2:F coated AISI446 stainless steels either at −0.1 V in 1 M H_2SO_4 + 2 ppm F^- at 70 °C purged with hydrogen gas or at 0.6 V in the solution purged with pressured air.

at *ca.* 9.0–15 μA cm^{-2} until 110 min of polarization when the current experiences a sharp increase. The current reaches *ca.* 4.45 mA cm^{-2} at the end of the test, clearly reflecting the poorer corrosion resistance of the modified coated AISI444 compared to the original coated AISI444. One would expect a lower anodic current for the coated steels in PEMFC cathode environment than in PEMFC anode environment, but this is not the case for these samples. Clearly additional work is needed to fully understand this result.

With a hydrogen gas purge, the original SnO_2:F coated AISI446 shows the sharpest current decay—a current drop immediately after polarization at −0.1 V (Fig. 7). Except for the current drop in the beginning of the test, the current is cathodic for the whole polarization period. A cathodic current indicates that the material is cathodically protected and anodic dissolution (corrosion) is in the equilibrium state, i.e., at the lowest possible (but not zero) rate. The current stays at *ca.* −1.0 to −3.5 μA cm^{-2} (negative indicating cathodic), and is extremely stable (Fig. 7). The same behavior was seen with thermally nitrided Ni–50Cr alloy and AISI446 steel in the same environment [21–23]. The potentiostatic polarization illustrates the superior performance of the original coated AISI446 in the PEMFC anode environment. On the other hand, the current decay for modified coated AISI446 seems not as sharp as that of the original coated one. Fig. 7 illustrates the current crossover to cathodic after *ca.* 10 min polarization for modified coated AISI446, which is one of the major differences from the original coated AISI446. The current is reasonably stable at *ca.* −3.0 to −8.0 μA cm^{-2} then, though cathodic current spikes is seen for the modified coated AISI446.

The original coated AISI446 has almost no current decay when polarized at 0.6 V. Extremely stable currents of *ca.* 0.2–1.0 μA cm^{-2} are seen in the whole test period, indicating excellent corrosion resistance in the PEMFC anode environment. On the other hand, it takes *ca.* 50 min for the modified coated AISI446 to stabilize under these conditions. Then the current is reasonably stable at *ca.* 4.0–6.0 μA cm^{-2}.

The above results again show the importance of the chemical composition of the substrate alloy on the performance of the SnO_2:F coated steels, with the original coated AISI446 still giving the best behavior in the simulated PEMFC environments. From the corrosion resistance point of view, the modified SnO_2:F coating process is not as good as original one.

3.4. Dissolved metal ions

The ICP analysis results for dissolved metal ions from the solutions after 7.5 h of potentiostatic polarization with fresh and SnO_2:F coated steels are shown in Table 1.

In general, Fe has the highest concentration in these solutions and Ni the lowest, almost at the detection limit of the ICP system. This is expected based on the steels' chemical composition and is in agreement with our previous XPS investigation on the passive film where Fe was selectively dissolved and Cr was enriched at the surface [11,30]. Solution samples tested with fresh AISI444 have the highest concentration of dissolved Fe, Cr and Ni. The heavy dissolution indicates that this bare alloy is not suitable for bipolar plates [10]. With the original SnO_2:F coating, dissolved Fe, Cr and Ni ions for coated AISI444 in the PEMFC cathode environment are 5 times less than the uncoated steel. Significant improvement is seen in the PEMFC anode environment for the original coated AISI444 where the dissolved Fe ion is over 11 times less and Cr over 18 times less than the uncoated sample. Also a few ppm of Sn were detected for original coated AISI444 in both PEMFC environments. These data confirm the corrosion protection of the original SnO_2:F coat-

Table 1
Fe, Cr, Ni ions concentration for bare and SnO_2:F coated stainless steels after 7.5 h polarization in PEMFC environments

Material	Ion content after 7.5 h in PEMFC anode (H_2) environment (ppm)				Ion content after 7.5 h in PEMFC cathode (air) environment (ppm)			
	Fe	Cr	Ni	Sn	Fe	Cr	Ni	Sn
AISI444	142	37.9	0.30		328	68.0	0.94	
SnO_2:F/AISI444(O)	12.7	2.09	–	1.76	64.4	13.7	0.22	4.50
SnO_2:F/AISI444(M)	30.4	6.39	–	2.26	134	30.0	0.39	9.52
AISI446	1.46	–	–		0.99	–	–	
SnO_2:F/AISI446(O)	1.24	–	–	–	0.98	–	–	–
SnO_2:F/AISI446(M)	2.13	0.27	–	0.18	2.07	0.33	–	0.12

O: original coated; M: modified coated.

ing on the steel. The modified SnO_2:F coating on AISI444 also lowers the dissolution of the metal ions as compared to the bare steel, though not as much as the original coating. In general, dissolved metallic ions for modified coated AISI444 are two to three times higher than those for original coated AISI444 in the same condition. With the modified SnO_2:F coating, dissolved Fe, Cr and Ni contents for coated AISI444 in the PEMFC cathode environment are decreased to less than half of the fresh steel in the same environment. Again, greater improvement is seen in the PEMFC anode environment for the modified coated AISI444 where the dissolved Fe ion is over 4 times less and Cr over 5 times less than the fresh sample under the same conditions.

Also note that there are more dissolved metal ions for fresh and coated AISI444 from the PEMFC cathode environment than from the anode one. This indicates that the PEMFC cathode environment is much more corrosive than the PEMFC anode environment for AISI444 steels, which is in excellent agreement with the potentiostatic polarization experiments (Fig. 6) where much higher anodic currents was registered in PEMFC cathode environment than in anode one. Since the PEMFC anode environment is reductive and the cathode environment is oxidative, one might expect lower anodic current for the steels in PEMFC cathode environment than in PEMFC anode environment. This is due to the expectation that the passive film of stainless steel should be more stable in the airside of the PEMFC. However, the experimental results from polarization curves and ICP analysis illustrate that this is not the case for AISI444 samples. Clearly additional work is needed to fully understand this behavior.

We determined previously that AISI446 was a good candidate steel for PEMFC environments [10]. The dissolved metallic ions, Table 1, give only ppm levels of Fe, confirming the low dissolution rate of the alloy and its high corrosion resistance in the PEMFC environments; thus the possible improvement by means of a coating is rather limited. Table 1 indicates that the dissolved Fe ions are more or less in the same level with or without the original SnO_2:F coating on AISI446, meaning that the improvement with original SnO_2:F coating is not significant for AISI446. On the other hand, in terms of corrosion resistance, Table 1 shows that the modified coated AISI446 doubles the Fe dissolution compared to the original coated AISI446. Trace Cr and Sn ions are also detected with the modified coated AISI446. This indicates that the corrosion resistance for the modified SnO_2:F coating on AISI446 is significantly reduced. Table 1 agrees well with the polarization curve in Fig. 7.

For both AISI444 and AISI446, the modified SnO_2:F coating process results in less corrosion resistance than the original coating, but improved ICR, which is the trade-off for applying this coating. An understanding of the mechanism for the enhanced corrosion from the modified process is necessary and improvements must be made before the coated steel can be used in a PEMFC bipolar plate application.

3.5. AES characterization

Fig. 8a shows an SEM image of the modified SnO_2:F coating on AISI444 steel. Grooves are from the polishing lines, which provided the crystallization base for the deposited film growth.

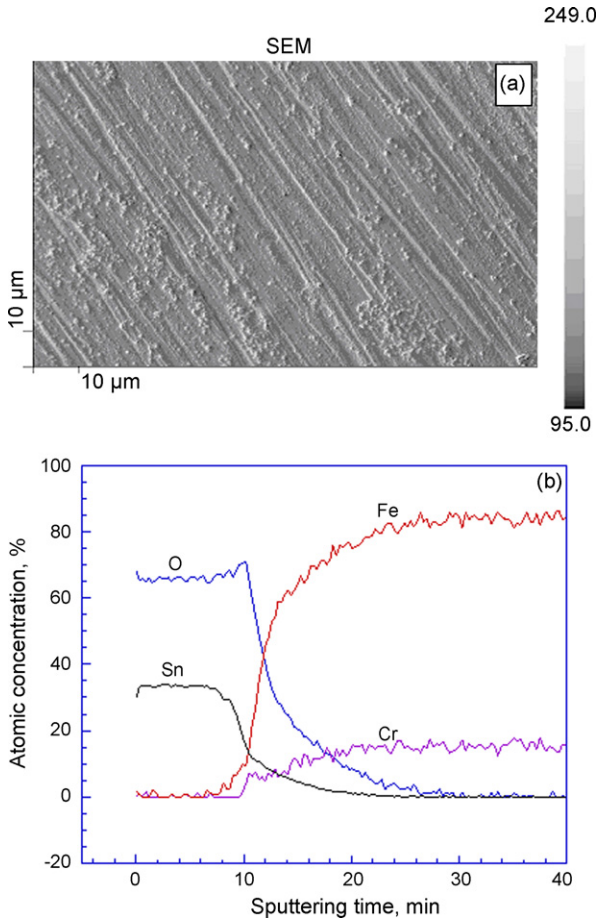

Fig. 8. (a) SEM image of the modified SnO_2:F coated AISI444 stainless steel. (b) AES depth profile for modified SnO_2:F coated AISI444 stainless steel.

Small particles of less than 1 μm diameter are common on the surface; these are clusters of crystals formed during the film growth. The AES depth profile for the modified coated AISI444 is shown in Fig. 8b. In the coated layer, only Sn and O are observed with a rough Sn:O ratio of 1:2. This gives the general chemical composition of the SnO_2 coating. Because F is added only as a dopant, its concentration does change the composition of the coating. The main steel compositional elements (Fe, Cr) appear at longer sputtering times. This is very similar to that of the original SnO_2:F coated steels [25,26]. Modified coated AISI446 has a similar image (not shown), and similar AES depth profile (not shown) except for the difference in the base metal content.

Using the half value of the O concentration as the boundary of the oxide and substrate steel, it took *ca.* 12.4 min to sputter off the oxide coating. Adopting a sputtering rate of 35 nm min^{-1}, the modified coating on AISI444 is *ca.* 0.43 μm thick. With the same procedure, the modified coating on AISI446 is estimated to be *ca.* 0.44 μm thick. Both agree well with each other and also with the original coating.

Fig. 9 illustrates the SEM image and the depth profile for modified coated AISI444 in the simulated PEMFC anode environment. Fig. 9a clearly shows that the surface coating is partially cracked or completely dissolved after 7.5 h of polariza-

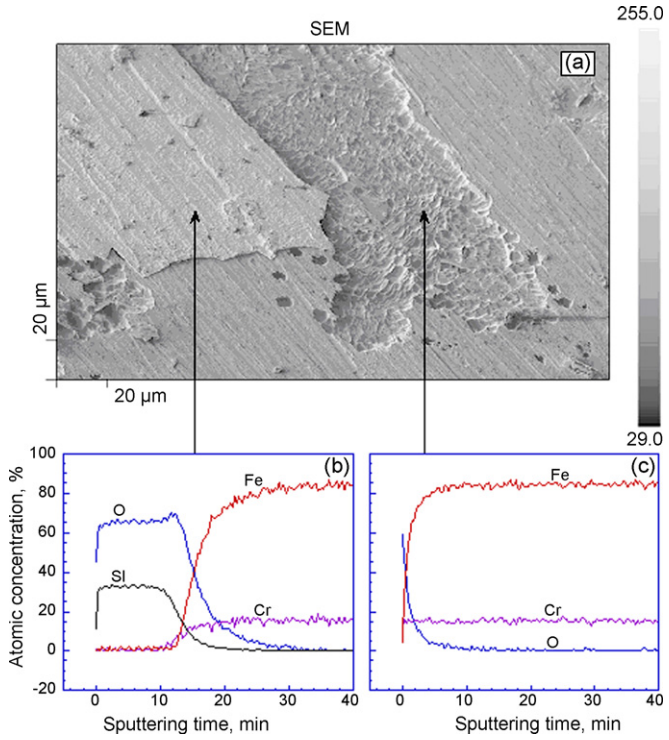

Fig. 9. (a) SEM image for the modified coated AISI444 steel after experienced 7.5 h polarization in PEMFC anode environment. (b) AES depth profile for covered area with the modified SnO_2:F coating as specified in (a). (c) AES depth profile for un-covered area as specified in (a).

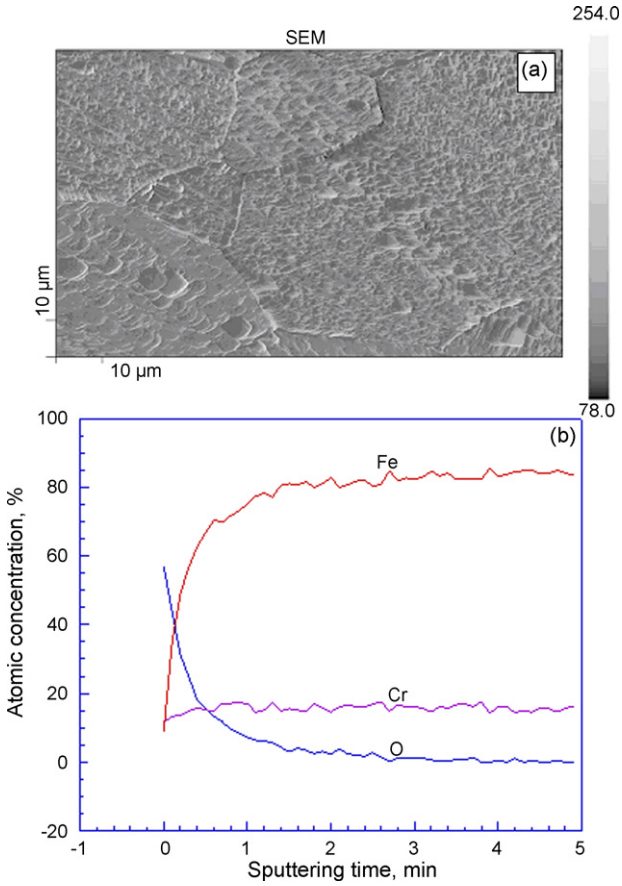

Fig. 10. (a) SEM image for the modified coated AISI444 steel after experienced 7.5 h polarization in PEMFC cathode environment. (b) AES depth profile for the modified coated AISI444 stainless steel after experienced 7.5 h polarization in PEMFC cathode environment.

tion. The leftover edges of the coating suggest that the modified coating flakes off, leaving large areas without the protection of the coating. This then becomes a pathway for corrosion attack. The area covered with modified coating gives an AES depth profile (Fig. 9b) identical to the freshly coated one (Fig. 8b). The area without coating coverage gives only metal and oxygen contents, without the surface SnO_2:F coating (Fig. 9c). This is a typical AES depth profile for a stainless steel, since it does not identify the metal valence.

Fig. 10a displays the SEM image for the modified coated AISI444 after experiencing 7.5 h of polarization in the simulated PEMFC cathode environment. We see that there is almost no coating coverage, leaving the surface without protection. Actually, the rough surface and the large grains can be easily observed from the image. The AES depth profile also gives only the metallic and oxygen contents (Fig. 10b, which is identical to Fig. 9c). Comparing Figs. 9 and 10, it is clear that the PEMFC cathode environment is more corrosive to the modified coated AISI444 than the PEMFC anode environment, which is in agreement with the potentiostatic polarization (Fig. 6) and the ICP analysis for the dissolved metallic ions (Table 1).

As mentioned before, the modified coated AISI446 has an image identical to that of coated AISI444, simply due to the same deposition procedure. The AES depth profile for the modified coated AISI446 reveals a similar plot, except for the composition of the base steels. The images for the modified coated AISI446 samples after 7.5 h of polarization in PEMFC anode and cathode environments are rather similar. Moreover, AES depth profiles are not affected by the environments. Fig. 11a presents a typical SEM image for the modified coated AISI446 in a simulated PEMFC anode environment. It is clear that some areas are covered by coating and some are not. Moreover, cracks are seen in the coating and this could be the reason for the area without coating. In this way, solution penetration at the cracks causes the coating to peel-off. Since such cracks are not seen in the freshly deposited samples, they must develop during the polarization process. Therefore, the adhesion of the modified coating might be the biggest challenge for the further modification.

The peeling-off of the coating during the polarization experiments generates bare areas among the coated areas. Somehow then, this is the reason for the observed higher dissolution rate for the modified coated AISI446 (Table 1). The area covered with modified coating gives an AES depth profile (Fig. 11b) identical to the freshly coated one, Fig. 8b. The area without coating coverage gives only metallic and oxygen contents, Fig. 11c. Fig. 11 is similar to Fig. 9, except that the un-covered area in Fig. 11 did not experience the heavy corrosion seen in Fig. 9. This is again due to the better corrosion resistance of the base AISI446 steel in these environments. Therefore, though the coating procedures on AISI444 and AISI446 are identical and the coatings have the same thickness and same uniformity, polarizations of the modi-

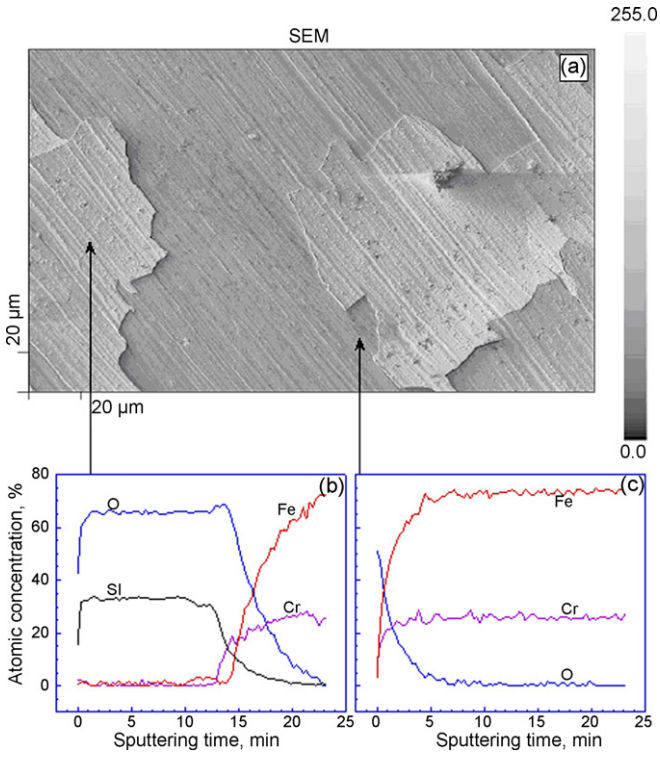

Fig. 11. (a) SEM image for the modified coated AISI446 steel after experienced 7.5 h polarization in PEMFC anode environment. (b) AES depth profile for covered area with the modified SnO_2:F coating as specified in (a). (c) AES depth profile for un-covered area as specified in (a).

fied coated steels in simulated PEMFC environments give very different profiles. This could be related to the possible pin-holes of the coatings. Fig. 8 shows surface clusters on the coating, which could be electrochemical active centers during the polarization process and thus pin-holes may be developed. When the electrolyte reaches the substrate through the pin-holes, the corrosion resistance of the substrate steel is then significant to the stability of the coated steel. Our experiments showed that bare AISI446 has excellent corrosion resistance in simulated PEMFC environments, while bare AISI444 steel has a poor behavior. The dark spots in the SEM image of Fig. 9 could be due to the pin-holes of the coating.

A possible explanation for the enhanced corrosion after the etch + coating process is that although the CBF_3 etching procedure removes the native oxide coating and increases the surface roughness, thus reducing the ICR, it leaves behind halide ion the form of Br^-. Originally the native oxide coating protects the bare metal from halide attack. However, in this case during the etching process halide can be left behind deposition directly on the bare steel. When the coating is compromised, halide-pitting corrosion is initiated and once that starts, the native oxide cannot form. One could certainly use a different etching procedure that did not involve halide, however the SnO_2:F deposition procedure requires it and it is not clear at this time how to get around this issue. Another possible investigation may involve the coating thickness. Thin coating may have less peel-off issues. However, the trade-off is that thin coating may also be less protective for steels like AISI444.

Anyway, the future automobile industry requires that the bipolar plate must be produced with high-speed and high-volume. Such pathways, like stamping, already exist for stainless steels. With these cost-effective materials, applying a coating of low ICR and corrosion resistance is one of the most promising methods for PEMFC bipolar plate application. Steels coated with SnO_2:F coating have been showing significant improvement both in ICR and corrosion resistance, though there still challenge in the adhesion of the coating. Similarly, some other thin film coating techniques, like atomic layered deposition (ALD) and plasma nitridation, should have possible applications in the fuel cell bipolar plates.

4. Conclusions

Our process for depositing the SnO_2:F coating was modified by means of a pre-etching step and applied to different stainless steel alloys with a coating thickness of *ca.* 0.43 μm. We determined that the substrate steel had a significant influence on the adhesion of the coating. Good coatings from the modified SnO_2:F deposition process were only obtained with ferrite stainless steels. The pre-etching modification of the SnO_2:F coating process decreased the ICR, a beneficial effect.

The modified coated AISI444 and AISI446 were characterized in 1 M H_2SO_4 + 2 ppm F^- at 70 °C purged either with hydrogen gas or pressured air, and their behavior compared with that of the original coated steels. Dynamic polarization experiments illustrated that the corrosion resistance of the modified coated steels is not as good as those with the original coating, though the substrate steel still plays an important role.

Potentiostatic polarization showed the same tendency. Modified coated AISI444 showed a reasonably stable current of *ca.* −7.0 to 1.0 μA cm^{-2} in a PEMFC anode environment, compared with *ca.* −1.0 to 4.0 μA cm^{-2} for original coated AISI444 in the same environment. In a PEMFC cathode environment, modified coated AISI444 has an increasing anodic current, reaching *ca.* 4.45 mA cm^{-2} at end of the test, which is much higher than the 1.40 mA cm^{-2} for original coated AISI444. It took *ca.* 10 min polarization for modified coated AISI446 to reach the cathodic stable current of −3.0 to −8.0 μA cm^{-2} in the PEMFC anode environment, compared with the −1.0 to −3.5 μA cm^{-2} for original coated AISI446 in the same condition. In the PEMFC cathode environment, the modified coated AISI446 needed *ca.* 50 min to stabilize at 4.0–6.0 μA cm^{-2}, compared with the 0.2–1.0 μA cm^{-2} for original coated AISI446. ICP analysis of the dissolved metallic ions is in agreement with the polarization. Both polarization and ICP analysis results indicate that the PEMFC cathode environment is more corrosive to the coated steels (especially AISI444) than the PEMFC anode environment. In terms of corrosion resistance in PEMFC environments, the modified coating is not as good as the original one.

The AES investigation also revealed that modified coated AISI444 experienced heavy dissolution in the PEMFC cathode environment, confirming that it is more corrosive than the PEMFC anode environment for the coated steels. Both coated AISI444 and coated AISI446 showed cracks and peel-off of the

modified coating after polarization. They are the sources for the higher anodic currents in the polarization curves compared to those of the original coated steels. The adhesion of the modified SnO_2:F coating is a challenge for the further research. Halide, especially bromide coming from the etching process, is suggested as the initiator of the higher corrosion rates observed in these simulated PEMFC environments. Removing the Br during the etching step is possible, but it still may be a problem during the SnO_2:F deposition process.

Acknowledgements

The authors thank Dr. Raghu Bhattacharya for the assistance in ICP analysis. This work was supported by the Hydrogen, Fuel Cell and Infrastructure Technologies Program of the US Department of Energy.

References

[1] B.C.H. Steele, A. Heinzel, Nature 414 (2001) 345.
[2] A. Hermann, T. Chaudhuri, P. Spagnol, Int. J. Hydrogen Energy 30 (2005) 1297.
[3] N. Huang, B. Yi, M. Hou, P. Ming, Prog. Chem. 17 (2005) 963.
[4] R.C. Makkus, A.H.H. Janssen, F.A. de Bruijn, R.K.A.M. Mallant, J. Power Sources 86 (2000) 274.
[5] D.P. Davies, P.L. Adcock, M. Turpin, S.J. Rowen, J. Power Sources 86 (2000) 237.
[6] R. Hornung, G. Kappelt, J. Power Sources 72 (1998) 20.
[7] S.-J. Lee, J.-J. Lai, C.-H. Huang, J. Power Sources 145 (2005) 362.
[8] A.K. Iversen, Corros. Sci. 48 (2006) 1036.
[9] H. Wang, M.A. Sweikart, J.A. Turner, J. Power Sources 115 (2003) 243.
[10] H. Wang, J.A. Turner, J. Power Sources 128 (2004) 193.
[11] H. Wang, G. Teeter, J.A. Turner, J. Electrochem. Soc. 152 (2005) B99.
[12] L. Ma, S. Warthesen, D.A. Shores, J. New Mater. Electrochem. Syst. 3 (2000) 221.
[13] J. Wind, R. Späh, W. Kaiser, G. Böhm, J. Power Sources 105 (2002) 256.
[14] A. Pozio, R.F. Silva, M. De Francesco, L. Giorgi, Electrochim. Acta 48 (2003) 1543.
[15] P.L. Hentall, J.B. Lakeman, G.O. Mepsted, P.L. Adcock, J.M. Moore, J. Power Sources 80 (1999) 235.
[16] J. Ihonen, F. Jaouen, G. Lindbergh, G. Sundholm, Electrochim. Acta 46 (2001) 2899.
[17] N. Cunningham, D. Guay, J.P. Dodelet, Y. Meng, A.R. Hlil, A.S. Hay, J. Electrochem. Soc. 149 (2002) A905.
[18] S. Joseph, J.C. McClure, R. Chianelli, P. Pich, P.J. Sebastian, Int. J. Hydrogen Energy 30 (2005) 1339.
[19] Y. Wang, D.O. Northwood, J. Power Sources 163 (2006) 500.
[20] M.P. Brady, K. Weisbrod, C. Zawodzinski, I. Paulauskas, R.A. Buchanan, L.R. Walker, Electrochem. Solid-State Lett. 5 (2002) A245.
[21] M.P. Brady, K. Weisbrod, I. Paulauskas, R.A. Buchanan, K.L. More, H. Wang, M. Wilson, F. Garzon, L.R. Walker, Scripta Mater. 50 (2004) 1017.
[22] H. Wang, M.P. Brady, G. Teeter, J.A. Turner, J. Power Sources 138 (2004) 86.
[23] H. Wang, M.P. Brady, K.L. More, H.M. Meyer III, J.A. Turner, J. Power Sources 138 (2004) 79.
[24] R. Tian, J. Sun, L. Wang, Int. J. Hydrogen Energy 31 (2006) 1874.
[25] H. Wang, J.A. Turner, X. Li, R. Bhattacharya, J. Power Sources 171 (2007) 567.
[26] H. Wang, J.A. Turner, J. Power Sources 170 (2007) 387.
[27] X. Li, T.A. Gessert, T. Coutts, Appl. Surf. Sci. 223 (2004) 138.
[28] R.N. Bhattacharya, A. Duda, D.S. Ginley, J.A. DeLuca, Z.F. Ren, C.A. Wang, J.H. Wang, Physica C 229 (1994) 145.
[29] Office of EERE: US DOE Hydrogen, Fuel Cells & Infrastructure Technologies Program, Multi-Year Research, Development and Demonstration Plan, website http://www1.eere.energy.gov/hydrogenandfuelcells/mypp/pdfs/fuel_cells.pdf.
[30] H. Wang, J.A. Turner, ECS Transactions, in: T. Fuller, C. Bok, C. Lamy (Eds.), Proton Exchange Membrane Fuel Cells V, in Honor of Supramaniam Srinivasan, vol. 1, No.6 (2006) pp. 263–272.